

## Organic Cation Permeation through the Channel Formed by Polycystin-2\*

Received for publication, April 21, 2005, and in revised form, June 8, 2005  
Published, JBC Papers in Press, June 16, 2005, DOI 10.1074/jbc.M504359200

Georgia I. Anyatonwu<sup>‡§</sup> and Barbara E. Ehrlich<sup>‡¶||</sup>

From the Departments of <sup>‡</sup>Pharmacology and <sup>¶</sup>Cellular and Molecular Physiology, Yale University School of Medicine, New Haven, Connecticut 06520

Polycystin-2 (PC2), a member of the transient receptor potential family of ion channels (TRPP2), forms a calcium-permeable cation channel. Mutations in PC2 lead to polycystic kidney disease. From the primary sequence and by analogy with other channels in this family, PC2 is modeled to have six transmembrane domains. However, most of the structural features of PC2, such as how large the channel is and how many subunits make up the pore of the channel, are unknown. In this study, we estimated the pore size of PC2 from the permeation properties of the channel. Organic cations of increasing size were used as current carriers through the PC2 channel after PC2 was incorporated into lipid bilayers. We found that dimethylamine, triethylamine, tetraethylammonium, tetrabutylammonium, tetrapropylammonium, and tetrapentylammonium were permeable through the PC2 channel. The slope conductance of the PC2 channel decreased as the ionic diameter of the organic cation increased. For each organic cation tested, the currents were inhibited by gadolinium and anti-PC2 antibody. Using the dimensions of the largest permeant cation, the minimum pore diameter of the PC2 channel was estimated to be at least 11 Å. The large pore size suggests that the primary state of this channel found *in vivo* is closed to avoid rundown of cation gradients across the plasma membrane and excessive calcium leak from endoplasmic reticulum stores.

Autosomal dominant polycystic kidney disease is a systemic hereditary disease characterized by renal and hepatic cysts that results in end-stage renal failure in 50% of affected individuals (1). This disease affects 1 of 800 live births (2). Most cases (>95%) are caused by genetic mutations in either the *PKD1* or *PKD2* gene, which encodes polycystin-1 (PC1)<sup>1</sup> and polycystin-2 (PC2), respectively (3).

\* This work was supported in part by National Institutes of Health grants. The costs of publication of this article were defrayed in part by the payment of page charges. This article must therefore be hereby marked "advertisement" in accordance with 18 U.S.C. Section 1734 solely to indicate this fact.

§ Supported by Yale University School of Medicine Pharmacology Training Grant T32-GM07324 and NIDDK, National Institutes of Health predoctoral fellowship 5F31DK062635.

¶ To whom correspondence should be addressed: Yale University School of Medicine, Dept. of Pharmacology, 333 Cedar St., New Haven, CT 06520. Tel.: 203-737-1188; Fax: 203-737-2027; E-mail: barbara.ehrlich@yale.edu.

<sup>1</sup> The abbreviations used are: PC, polycystin; RyR, ryanodine receptor; DMA, dimethylamine; TriEA, triethylamine; TEA, tetraethylammonium; TBA, tetrabutylammonium; TPA, tetrapropylammonium; TPpEA, tetrapentylammonium; TRP, transient receptor potential; TRPV6, transient receptor potential vanilloid 6 receptor; TAA, tetraalkylammonium; CHAPS, 3-[(3-cholamidopropyl)dimethylammonio]-1-propanesulfonic acid; TriMA, trimethylamine; MTSEA, methanethiosulfonate ethylammonium; IP<sub>3</sub>R, inositol 1,4,5-trisphosphate receptor; ER, endoplasmic reticulum.

PC1 is a 4302-amino acid integral membrane protein with an extracellular N terminus of ~3000 residues, which contains a novel combination of known motifs originally found in other proteins that are involved in cell-cell and cell-matrix interactions (4). PC2 is a 968-amino acid integral membrane protein that functions as a calcium-permeable cation channel (5, 6). PC2 (also called TRPP2) belongs to the family of transient receptor potential (TRP) channels (7). PC1 and PC2 co-assemble through their coiled-coil domains (8, 9). Because many of the pathogenic mutations are in the interacting domains, the co-assembly of PC1 and PC2 is thought to be essential for the function of these proteins in kidney.

PC2 is a nonselective cation channel with multiple subconductance states and a high permeability to calcium (5). PC2 is also permeable to monovalent cations such as Na<sup>+</sup>, Cs<sup>+</sup>, and K<sup>+</sup> and divalent cations such as Ba<sup>2+</sup> and Mg<sup>2+</sup>, but it is more permeable to divalent than to monovalent cations (5, 6). This channel is activated at low concentrations of calcium and inhibited at high concentrations of calcium (6). Other inhibitors include lanthanum (La<sup>3+</sup>), gadolinium (Gd<sup>3+</sup>), amiloride, and a reduction in pH (5).

PC2 comprises six transmembrane-spanning domains where both the C and N termini are intracellular. The fifth and sixth transmembrane domains of PC2 are similar to those of the voltage-gated potassium channels (K<sub>v</sub>) and are hypothesized to form the pore region (10). It is still unknown how many subunits make up the pore of the PC2 channel. The ion selectivity differs between K<sub>v</sub>, which is highly potassium-selective, and PC2, which does not select among the cations. To investigate this difference, we examined the permeation properties of PC2. In previous reports, organic cations with known ionic diameters were employed to determine the pore diameters of ion channels such as the ryanodine receptor (RyR), potassium channel KcsA, and the vanilloid receptor (TRPV6) (11–14). These previous reports revealed that the RyR has one pore of a minimum diameter of ~7 Å (13). TRPV6, which belongs to the family of TRP channels, has a minimum pore diameter estimated to be ~5.4 Å (14). RyR and TRPV6 are highly permeable to calcium and exhibit greater permeability for divalent cations compared with monovalent cations, which are biophysical characteristics similar to those of PC2 channels (14). Unfortunately, the pore size of PC2 cannot be inferred from the some of the aforementioned biophysical properties.

To estimate the pore size of the PC2 channel, we used a series of organic cations with varying ionic diameters. Organic amines such as dimethylamine (DMA<sup>+</sup>) and triethylamine (TriEA<sup>+</sup>) and large tetraalkylammonium (TAA<sup>+</sup>) derivatives such as tetraethylammonium (TEA<sup>+</sup>), tetrabutylammonium (TBA<sup>+</sup>), tetrapropylammonium (TPA<sup>+</sup>), and tetrapentylammonium (TPpEA<sup>+</sup>) were used as current carriers through the PC2 channel after incorporation of the channel into planar lipid bilayer membranes. The currents carried by these organic cat-

ions through PC2 were inhibited by  $Gd^{3+}$ , an antagonist of PC2, and also by anti-PC2 antibody. These data show that the PC2 channel pore is able to accommodate large organic cations such as  $TBA^+$  and  $TPEA^+$ . From our results, we conclude that PC2 has a minimum pore diameter greater than 11 Å, a diameter that is nearly twice that of the RyR or TRPV6.

#### EXPERIMENTAL PROCEDURES

**Materials**—All chemicals were purchased from Sigma-Aldrich. Chloride salts of the organic cations were used.

**Planar Lipid Bilayer Measurements**—Membrane vesicles enriched in ER from LLC-PK<sub>1</sub> porcine kidney cell lines stably expressing PC2 (6, 15) were isolated by differential centrifugation in the presence of protease inhibitors (16). Vesicles enriched in ER membranes were fused to lipid bilayers containing phosphatidylethanolamine and phosphatidylserine (3:1 w/w; Avanti Polar Lipids, Alabaster, AL) dissolved in decane (40 mg lipid  $ml^{-1}$ ) (17). In experiments using  $Cs^+$  as the primary current carrier, ER membranes containing PC2 were added to the *cis* side, which contained 500 mM CsCl, 7  $\mu$ M  $CaCl_2$ , and 10 mM HEPES, 0.2 mM EGTA, pH 7.35, and the *trans* side, which contained 250 or 50 mM CsCl, 10 mM HEPES, pH 7.35. After fusion of vesicles, the *cis* side was rapidly perfused with 15 ml of the *trans* buffer with no added calcium. In all experiments single-channel currents were measured at various holding potentials with respect to the *trans* (ground) side.

In experiments using organic amines and large  $TAA^+$  derivatives as the current carrier, ER vesicles were fused to the bilayer in the presence of  $Cs^+$  as described above, but the  $TAA^+$  was in the *trans* compartment. For current-voltage experiments performed under asymmetrical conditions, organic amines or  $TAA^+$  (250 mM amine or  $TAA^+$ , 10 mM HEPES, pH 7.35) were present on the *trans* side, and the *cis* buffer comprised 250 mM CsCl, 10 mM HEPES, pH 7.35. In experiments using gadolinium ( $Gd^{3+}$ ) to modify the cesium currents,  $Gd^{3+}$  (0–500  $\mu$ M) was added to the *cis* side for the concentration dependence. Subsequent experiments were performed at 400  $\mu$ M  $Gd^{3+}$ . In experiments using anti-PC2 antibody, a 1:350 dilution of anti-PC2 antibody was added to the *cis* side. This antibody was generated using a 275-amino acid peptide from the C-terminal portion of PC2 (15).

**Analysis of Current Amplitudes**—Data were amplified (BC-525C, Warner Instruments, Hamden, CT), filtered at 1–3 kHz with a low-pass eight-pole Bessel filter, digitized at 10 kHz, (Digidata 1322, Axon Instruments, Foster City, CA), and stored on a personal computer. Subsequent data analysis was performed using pCLAMP (Axon Instruments). Current amplitudes for the current-voltage relationships as shown in Fig. 2A were generated using all-points histograms for each current carrier. All-points histograms were generated from at least 2 s of continuously recorded data and fit with a Gaussian curve. Open channel current amplitudes were collected for each cation tested. The junction potentials were factored into all of the current amplitude analyses performed.

Current amplitudes were calculated as the difference between the Gaussian means of the open and closed states. Errors shown in the figures were derived using the standard deviations from the Gaussian fit described above. Permeability ratios relative to  $Cs^+$  ( $P_x/P_{Cs}$ ) were calculated from the asymmetrical reversal potentials (18). The slope conductance was determined by fitting a linear regression line through holding potentials ranging from –10 to –60 mV. A graph was plotted of slope conductance versus the minimum ionic diameter of the cations, and points were fit to an exponential equation. All representative current traces shown in the figures were filtered at 500 Hz and are at least 500 ms long.

**Western Blot**—Membrane vesicles derived from LLC-PK<sub>1</sub> cells were solubilized with 1% CHAPS for 1 h under constant agitation at 4 °C. Samples were collected and centrifuged at 10,000 rpm for 15 min at 4 °C. Protein concentration was determined using the Bradford assay (Pierce). 50  $\mu$ g of supernatant sample was added to 2 $\times$  Laemmli buffer containing 5%  $\beta$ -mercaptoethanol, and the proteins were resolved on 4–20% SDS polyacrylamide gels at 200 mV for 4–5 h. Proteins were transferred to a polyvinylidene difluoride membrane at 30 mV and 250 mA for 18–20 h at 4 °C. The polyvinylidene difluoride membrane was blocked with 1 $\times$  phosphate-buffered saline (containing 0.5% Tween 20 and 5% nonfat milk powder) and incubated with primary antibodies anti-RyR (clone MA3-925; Affinity BioReagents) at 1:1,000 for 2 h or anti-calnexin antibody (Stressgen, Victoria, British Columbia, Canada) at 1:2,000 for 1 h. Secondary antibodies used were either anti-mouse or anti-rabbit horseradish peroxidase-conjugated antibodies at 1:40,000 for 1 h. Samples were visualized using enhanced chemiluminescence detection reagents (Amersham Biosciences). Representative results of at least three independent experiments are shown.

TABLE I  
Diameter of current carriers

Values were obtained from Refs. 22 and 44.

Current carriers	Formula	Diameter
		Å
Cesium( $Cs^+$ )	$Cs^+$	3.4
DMA <sup>+</sup>	$(CH_3)_2NH_2^+$	4.6
TriEA <sup>+</sup>	$(C_2H_5)_3NH^+$	7.2
TEA <sup>+</sup>	$(C_2H_5)_4N^+$	6.1–8.2 <sup>a</sup>
TPA <sup>+</sup>	$(C_3H_7)_4N^+$	9.8
TBA <sup>+</sup>	$(C_4H_9)_4N^+$	9.5–11.6 <sup>a</sup>
TPEA <sup>+</sup>	$(C_5H_{11})_4N^+$	11.1–13.2 <sup>a</sup>

<sup>a</sup> Indicates the maximum diameter of cation.

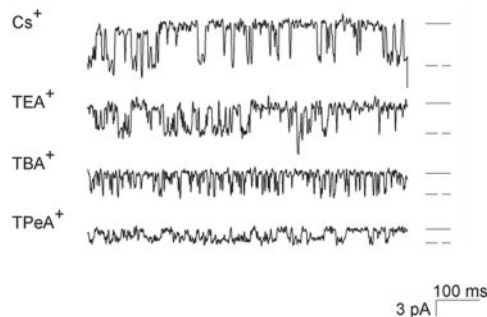


FIG. 1. Current traces of cations tested. Downward deflections are channel openings. Top trace,  $Cs^+$  currents; second trace, TEA<sup>+</sup> currents; third trace, TBA<sup>+</sup> currents; fourth trace, TPEA<sup>+</sup> currents. Experiments were performed under asymmetrical conditions (250 mM CsCl on the *cis* side, 250 mM amine or  $TAA^+$  on the *trans* side). All representative current traces shown in this figure were obtained at –40 mV, filtered at 400 Hz. To the right of each trace, the open state is represented by a dashed line, and the closed state by a solid line.

#### RESULTS

**Conductance through PC2 Channels by Organic Cations**—The organic amines DMA<sup>+</sup> and TriEA<sup>+</sup> and the large tetraalkylammonium derivatives TEA<sup>+</sup>, TBA<sup>+</sup>, TPA<sup>+</sup>, and TPEA<sup>+</sup> were used to probe the pore of the PC2 channel. The ionic diameters of these organic cations are shown in Table I.  $Cs^+$ , which has the smallest diameter (3.4 Å), was used as the cation for comparisons. There is some variation in the diameters of several of the  $TAA^+$  derivatives because the alkyl chains can be flexible with free rotation occurring around their carbon-carbon bonds.

Fig. 1 shows a recording of single-channel currents for some of the organic cation used at a fixed holding potential under asymmetric conditions ( $Cs^+$  on the *cis* side, test cation on the *trans* side). The relative difference in current amplitude among the test cations (DMA<sup>+</sup>, TriEA<sup>+</sup>, TEA<sup>+</sup>, TBA<sup>+</sup>, TPA<sup>+</sup>, and TPEA<sup>+</sup>) was measured under asymmetrical conditions at holding potentials ranging from 0 to –60 mV (Fig. 2A). The current amplitude decreased as the ionic diameter of the current carrier increased (Fig. 2A). This observation is similar to that seen when organic amines of varying sizes conduct through the intracellular calcium channel, the RyR (11, 13, 19).

The trend in current amplitudes is also reflected in the reversal potentials and permeability ratios obtained for each cation (Table II). The reversal potential for the cations decreases as the ionic diameter of the cation changes (Table II). Although TPA<sup>+</sup> (9.8 Å) has a slope conductance similar to TBA<sup>+</sup> (9.5–11.6 Å), it appears to be more permeable through PC2 than TBA<sup>+</sup>; however, the reversal potential of TBA<sup>+</sup> is smaller. This may be due to the flexibility of TBA<sup>+</sup>, where the diameter has been calculated to vary between 9.5 and 11.6 Å. Interestingly, the similarity of the currents by the least permeable cations, TBA<sup>+</sup> and TPEA<sup>+</sup> (Table II), implies that the diameter of TBA<sup>+</sup> being “sensed” in our experiments may actually be closer to 11.6 Å. From the permeability ratios, it is

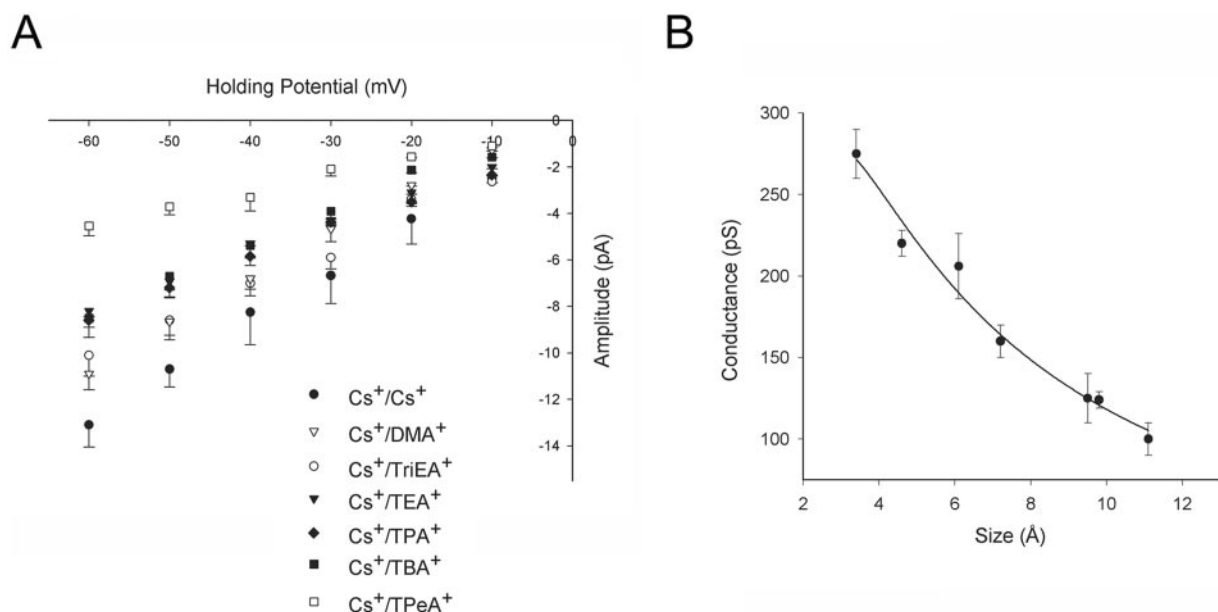


FIG. 2. **Current amplitude and slope conductance of each cation tested under asymmetrical conditions.** A, current-voltage relationship of cations. The current amplitudes for Cs<sup>+</sup> (●, *n* = 3), DMA<sup>+</sup> (▽, *n* = 4), TriEA<sup>+</sup> (○, *n* = 4), TEA<sup>+</sup> (▼, *n* = 4), TPA<sup>+</sup> (◆, *n* = 4), TBA<sup>+</sup> (■, *n* = 4), and TPeA<sup>+</sup> (□, *n* = 4) were obtained at holding potentials ranging from 0 to -60 mV. Each point is the average of >100 channel openings. B, slope conductance of cations as a function of the ionic diameter of each cation. The slope conductance for each cation was obtained from the current-voltage relationship shown in A. Error bars represent the S.E.

clear that all of the cations tested permeate through PC2. The slope conductance measured from single-channel current amplitudes at negative holding potentials under asymmetrical conditions also decreased as the size of the cation increased (Fig. 2B). The largest slope conductance of 275 ± 15 picosiemens was found for Cs<sup>+</sup>, the most permeant cation. The slope conductance (in picosiemens for each cation) for DMA<sup>+</sup> and TriEA<sup>+</sup> are 220 ± 8 and 206 ± 20; TEA<sup>+</sup> and TBA<sup>+</sup> are 160 ± 10 and 125 ± 15; TPA<sup>+</sup> and TPeA<sup>+</sup> are 124 ± 5 and 100 ± 10 (Table II).

**Inhibition of Cation Currents through PC2 by Gadolinium—** Previous studies have shown that the PC2 channel is inhibited by Gd<sup>3+</sup> (5). In this series of experiments, we used Gd<sup>3+</sup> solely to determine whether the cation currents we observed are through PC2. We first examined the effect of Gd<sup>3+</sup> on the Cs<sup>+</sup> current. The concentration dependence of channel block by Gd<sup>3+</sup> was determined to identify the concentration needed for complete inhibition of channel activity. This concentration then was used to inhibit the currents carried by the test cations. Gd<sup>3+</sup> inhibited PC2 channel activity by decreasing the channel open probability with an IC<sub>50</sub> of 206 μM and full inhibition at 400 μM (Fig. 3). The concentration of Gd<sup>3+</sup> needed to inhibit the PC2 channel is similar to that used to inhibit TRP channels, further strengthening the structural similarity between PC2 and TRP channels (20). Concentrations of Gd<sup>3+</sup> that partially blocked PC2 channel activity showed no effect on the single-channel conductance. Gd<sup>3+</sup> failed to inhibit Cs<sup>+</sup> currents when it was added to the *trans* side (Fig. 3B).

The effect of Gd<sup>3+</sup> was tested to determine whether the currents carried by each of the test compounds were passing through the PC2 channel. Addition of 400 μM Gd<sup>3+</sup> inhibited currents carried by the test cations; representative recordings using DMA<sup>+</sup>, TEA<sup>+</sup>, TBA<sup>+</sup>, and TPeA<sup>+</sup> are shown (Fig. 4). The effect of Gd<sup>3+</sup> on all of the cations tested, including Cs<sup>+</sup>, was reversible upon perfusion of the recording chamber with buffer lacking the inhibitor. These results show that the currents carried by the test compounds are through the PC2 channel.

We also utilized anti-PC2 antibody to inhibit the channel because Gd<sup>3+</sup> can inhibit other ion channels. Channel activity

TABLE II  
*Slope conductance and reversal potential of current carriers*  
Values for the conductance were taken from experiments shown in Fig 2. All reversal potentials were corrected for junction potentials. pS, picosiemens.

Current carriers	Slope conductance pS	V <sub>rev</sub> mV	P <sub>x</sub> /P <sub>Cs</sub>
Cs <sup>+</sup>	275 ± 15	0	0
DMA <sup>+</sup>	220 ± 8	-1.1 ± 0.1	0.96
TriEA <sup>+</sup>	206 ± 20	-2.8 ± 0.1	0.90
TEA <sup>+</sup>	160 ± 10	-3.9 ± 0.3	0.86
TPA <sup>+</sup>	124 ± 5	-9.8 ± 0.4	0.69
TBA <sup>+</sup>	125 ± 15	-15.1 ± 0.9	0.59
TPeA <sup>+</sup>	100 ± 10	-12.2 ± 0.6	0.60

was observed at -40 mV, and then the antibody was added to the *cis* side. When the current was carried by Cs<sup>+</sup>, DMA<sup>+</sup>, TEA<sup>+</sup>, or TBA<sup>+</sup>, channel activity was inhibited after addition of the antibody (Fig. 5). Addition of preimmune serum had no effect on PC2 channel activity (data not shown). These results are similar to those obtained with Gd<sup>3+</sup>, supporting our assumption that the activity of PC2 was responsible for the measured currents.

The PC2 channels used for these measurements were from ER membranes that could contain additional calcium-permeable channels, specifically the RyR or the inositol 1,4,5-trisphosphate receptor (IP<sub>3</sub>R). An immunoblot of samples from vesicles derived from LLC-PK<sub>1</sub> cells using an anti-RyR antibody that recognizes all three RyR subtypes showed that the vesicles do not express the RyR (565 kDa) (Fig. 6). The same immunoblot was reprobed for the ER resident protein calnexin (90 kDa) to show that similar amounts of samples were loaded (Fig. 6). The IP<sub>3</sub>R is present in LLC-PK<sub>1</sub> cells, but it was not activated because of the absence of its agonist, IP<sub>3</sub>, during the experiments. From these results, we conclude that the currents observed were not carried by the RyR or IP<sub>3</sub>R. In addition to possibly harboring these other intracellular channels, LLC-PK<sub>1</sub> may also contain endogenous PC1 (15, 21). PC1 is expressed in the plasma membrane, and plasma membrane proteins such as the epidermal growth factor receptor and the

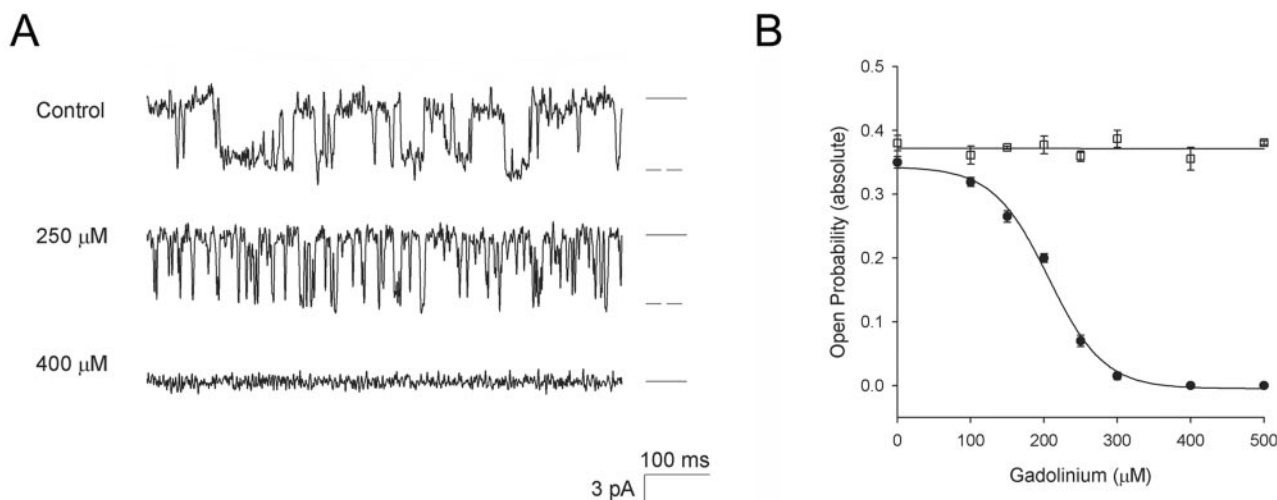


FIG. 3. **Gadolinium inhibits Cs<sup>+</sup> currents through PC2.** A, Cs<sup>+</sup> current traces are shown in the presence of 0 (Control), 250, and 400 μM Gd<sup>3+</sup>. Experiments were performed under symmetrical conditions (250 mM CsCl in both the *cis* and *trans* sides). All representative current traces shown were obtained at -40 mV, filtered at 400 Hz. Downward deflections are channel openings. To the *right* of each trace, the open state is represented as a *dashed line*, and the *solid line* represents the closed state. B, dose-dependent inhibition of the open probability of the PC2 channel by Gd<sup>3+</sup>. Experiments were conducted with Gd<sup>3+</sup> ( $n = 3$ ) added to the *cis* (●) or the *trans* side (□). Note that Gd<sup>3+</sup> had no effect on the open probability of the PC2 channel when added to the *trans* side. Error bars represent the S.E.

FIG. 4. **Gadolinium block of organic cation currents through PC2.** Currents obtained in the absence of Gd<sup>3+</sup> are shown on the *left*, and currents obtained in the presence of 400 μM Gd<sup>3+</sup> are shown on the *right*. Experiments were performed under symmetrical conditions (250 mM cation in both the *cis* and *trans* sides;  $n = 3$ ). Downward deflections represent channel openings. Currents for DMA<sup>+</sup>, TEA<sup>+</sup>, TBA<sup>+</sup>, and TPeA<sup>+</sup> were obtained at a holding potential of -40 mV, filtered at 400 Hz. To the *right* of each trace, the open state is represented by a *dashed line* and the closed state by a *solid line*.

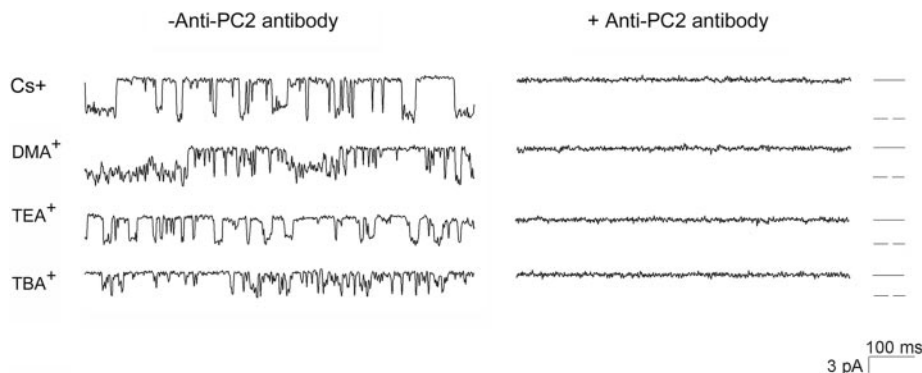
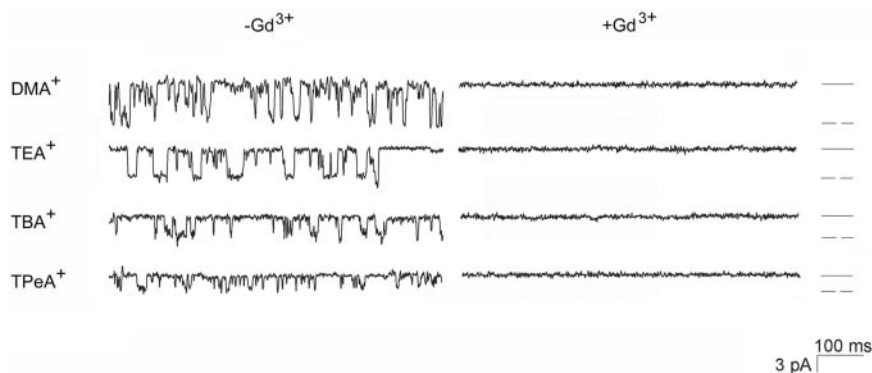


FIG. 5. **Anti-PC2 antibody inhibits PC2 channel activity.** Currents obtained in the absence of anti-PC2 antibody are shown on the *left*, and currents obtained in the presence of anti-PC2 antibody (1:350 dilution) are shown on the *right*. Experiments were performed under symmetrical conditions (250 mM cation on both the *cis* and *trans* sides;  $n = 3$ ). Downward deflections represent channel openings. Currents for Cs<sup>+</sup>, DMA<sup>+</sup>, TEA<sup>+</sup>, and TBA<sup>+</sup> were obtained at a holding potential of -40 mV, filtered at 400 Hz. To the *right* of each trace, the open state is represented by a *dashed line*, and the closed state by a *solid line*.

sodium hydrogen exchanger-3 were previously shown to be removed from the ER fraction of the kidney tissue lysate (6). Therefore, PC1 should not influence the activity of PC2 channels derived from the ER microsomes preparations.

#### DISCUSSION

In this study, we examined the pore size of the PC2 channel. The conductance of a series of organic cations of increasing diameter through PC2 was used to address this question. Six organic cations (dimethylamine, triethylamine, tetraethylammonium, tetrabutylammonium, tetrapropylammonium, and tetrapentylammonium) were selected because they spanned a range of molecular sizes and consequently a range of conduc-

tances through the PC2 channel. We found the following: 1) the PC2 channels are permeable to large organic cations; 2) the slope conductance of the PC2 channel decreased as the ionic diameter of the cations increased; and 3) PC2 channel currents carried by the organic cations were inhibited by Gd<sup>3+</sup>, a known inhibitor of PC2 (5). The observation that very large cations such as TPeA<sup>+</sup> were able to conduct through PC2 shows that the conduction pathway of PC2 is able to accommodate ions with a diameter up to at least 11 Å. TPeA<sup>+</sup> was the largest cation used in our experiments because tetraalkylammonium derivatives larger than TPeA<sup>+</sup> were insoluble in water making it impossible to conduct comparable electrophysiological measurements.

The findings in the present study highlight the inherent differences between the biophysical properties of PC2 and other calcium channels such as the RyR and TRP channels. With the RyR, three main differences can be highlighted. The first difference is the permeation properties of large tetraalkylammonium derivatives. In the RyR, organic amines such as trimethylamine ( $\text{TriMA}^+$ ) were used to show that it had a minimum pore diameter of  $\sim 7 \text{ \AA}$  (22). However, large tetraalkylammonium derivatives such as  $\text{TEA}^+$ ,  $\text{TPA}^+$ , and  $\text{TPeA}^+$  are impermeant through RyR and inhibit conduction of  $\text{K}^+$  through RyR in a voltage-dependent manner (23). The blocking effect of these derivatives was only observed when added to the *cis* side but not the *trans* side of the bilayer (23). Unlike RyR, these large cations conduct through the PC2 channel (see Figs. 1 and 2). It is interesting to note that  $\text{Cs}^+$  has a higher slope conductance for the RyR than the PC2 channel suggesting that  $\text{Cs}^+$  is more permeable through the RyR than through the PC2 channel (Fig. 7). However, the curve relating the slope conductance and the diameter of the test cations drops off more quickly for the RyR than for the PC2 channel. In addition,  $\text{TriEA}^+$  ( $7.2 \text{ \AA}$ ) is impermeant through RyR (22), whereas this and several even larger cations are still able to permeate through the PC2 channel as shown in our experiments. This comparison shows that the pore size and permeability characteristics of the PC2 channel are drastically different from those of the RyR.

The second difference between the two ion channels is the sensitivity to inhibition by  $\text{Gd}^{3+}$ . The concentration needed to achieve half-block of the PC2 channel is  $206 \mu\text{M}$ , and full inhibition occurred at  $400 \mu\text{M}$  (Fig. 3). In contrast, full inhibition of the RyR occurred at  $10 \mu\text{M}$  (24). The concentration of  $\text{Gd}^{3+}$  needed to block PC2 is more in line with that needed to inhibit other members of the TRP family (20).

The third difference between the two ion channels is modification of cationic current by methanethiosulfonate ethylammonium ( $\text{MTSEA}^+$ ).  $\text{MTSEA}^+$  is known to covalently modify cysteine residues within the conduction pathway of various ion channels such as the acetylcholine receptor, potassium channels, and the  $\gamma$ -aminobutyric acid type A receptor (25–27). Previous work using RyR showed that  $\text{MTSEA}^+$  could modify and irreversibly inhibit the current amplitudes of monovalent and divalent cations such as  $\text{MA}^+$ ,  $\text{DMA}^+$ ,  $\text{EA}^+$ ,  $\text{TriMA}^+$ , and  $\text{Ba}^{2+}$  (11, 28). In contrast, we found that  $\text{MTSEA}^+$  has no effect on PC2 at concentrations shown to inhibit RyR (data not shown). The basis for this discrepancy is not clear. It is possible that the number of cysteines available for modification in PC2 is reduced compared with those in RyR. Indeed this appears to be the case because the RyR is postulated to have 80–100 cysteines/subunit, where  $\sim 25\%$  of them are accessible for covalent modification by  $\text{MTSEA}^+$ , and the remaining are unavailable because they do not reside on the surface of the protein, or they form intraprotein disulfide bonds (29). On the other hand, the sequence of PC2 shows that this channel has only 12 cysteine residues. Although the surface availability of these cysteines is unknown, none of them is located in the putative pore-forming regions of the fifth and sixth transmembrane domains (30).

Although PC2 belongs to the family of TRP channels (7), its permeation/pore properties are distinct from TRP channels. The pore of TRP channels has not been well studied; however, a recent report (14) focusing on TRPV6 (vanilloid receptor) revealed, using organic cations such as  $\text{MA}^+$ ,  $\text{DMA}^+$ ,  $\text{TriMA}^+$ , tetramethylammonium, and *N*-methyl-*D*-glucamine, that its pore diameter is  $\sim 5.4 \text{ \AA}$ . TRPV6 has very low or zero permeability to  $\text{TriMA}^+$  ( $5.2 \text{ \AA}$ ) and tetramethylammonium ( $5.8 \text{ \AA}$ ), respectively (14). Another difference is in the effect of the divalent cation,  $\text{Mg}^{2+}$ , on both channels.  $\text{Mg}^{2+}$  ( $2 \text{ mM}$ ) can block

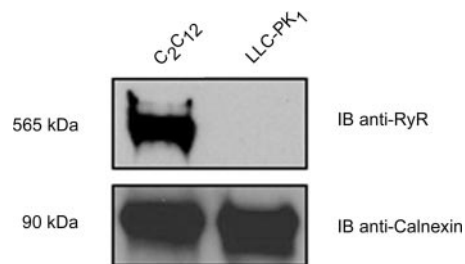


**FIG. 6. LLC-PK<sub>1</sub> cells lack RyR expression.** Protein samples were prepared from membrane vesicles derived from LLC-PK<sub>1</sub> cells. Samples were resolved on SDS-PAGE and either immunoblotted with anti-RyR antibody (upper panel) or anti-calnexin antibody (lower panel). C<sub>2</sub>C<sub>12</sub> (a mouse skeletal myogenic cell line, which contains all subtypes of the RyR (43), was used as a positive control in this experiment. The lower panel represents a reprobe of the same samples with anti-calnexin antibody.

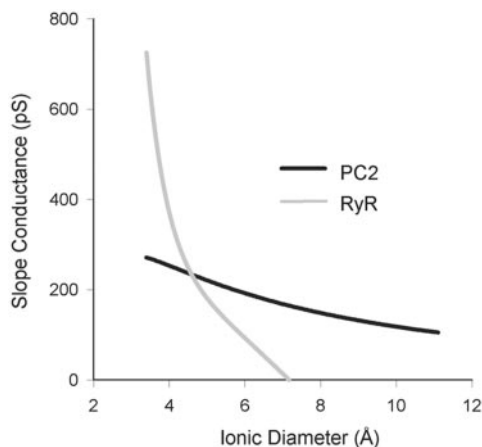


**FIG. 7. Slope conductance curves for PC2 and RyR.** The black line represents the relationship between the slope conductance and the ionic diameter of the current carrier for PC2, and the gray line represents the relationship for the RyR. The curve for PC2 was obtained from values in Table II. The curve for RyR was obtained from previously published values for the slope conductances and ionic diameters of  $\text{Cs}^+$ , methylamine,  $\text{DMA}^+$ , ethylamine,  $\text{TriMA}^+$ , and triethylamine (11, 13).

and unblock TRPV6 in a voltage-dependent manner (31), whereas  $\text{Mg}^{2+}$  ( $55 \text{ mM}$ ) permeates through PC2 and exhibits no inhibitory effect on PC2 (6). Although differences exist in the pore diameter of these related channels, they produce similar responses to  $\text{MTSEA}^+$ . Wild-type TRPV6 is resistant to modification by  $\text{MTSEA}^+$  (14), as is PC2. However, currents through TRPV6 could be blocked by  $\text{MTSEA}^+$  after introducing cysteines in the putative pore-lining domains (14). These observations further support the comparisons between the fifth and sixth transmembrane domains as pore-lining domains of TRP and PC2 channels.

Ion channels similar to PC2 that have large pore diameters include MthK (a calcium-activated potassium channel) (12, 32) and the colicin E1 receptor (33). MthK has previously been used as a model protein to understand the structure-function relationships of  $\text{K}^+$  channels and is structurally similar to the P-loop of KcsA, the region of the protein thought to be critical for formation of the MthK pore (12, 32, 34). Unlike KcsA, which has a pore diameter of  $4 \text{ \AA}$ , MthK has a pore diameter of  $\sim 12 \text{ \AA}$  at its narrowest point (32). Coincidentally, the MthK pore has a diameter that can accommodate the cations  $\text{TBA}^+$  and  $\text{TPeA}^+$ , both of which permeate through the PC2 channel. The colicin E1 receptor is an antibacterial toxin that forms voltage-dependent channels when inserted into lipid bilayer membranes (33). Interestingly, the colicin E1 receptor has a pore diameter that supports currents carried by nicotine adenine

dinucleotide (NAD<sup>+</sup>), a cation with a diameter of 12–16 Å (33). Thus, the PC2 pore size of at least 11 Å is larger than most calcium and potassium channels but reminiscent of MthK and the colicin E1 receptor.

When compounds of known sizes can pass through an ion channel, it is possible to calculate the number of transmembrane helices needed to form the pore. For the RyR, TRP, and K<sup>+</sup> channels it has been proposed that two transmembrane domains (S5 and S6) are contributed from each subunit (35–37). With the tight packing of the transmembrane domains shown for the K<sup>+</sup> channels (38) and similar tight packing expected for the RyR, at least eight transmembrane helices are needed to form such a large pore (37). Assuming that a minimum of eight transmembrane domains are needed and presuming that the same two transmembrane domains (S5 and S6) are contributed to form the pore (as in RyR/IP<sub>3</sub>R/TRP), then our present experiments suggest a tetrameric assembly of the PC2 protein. Intriguingly, using biochemical techniques, PC2 has been shown to homodimerize in solution (10); however, it is not known whether the dimers associate in its native environment.

The results presented here also strongly suggest that the PC2 channel must be in the closed conformation most of the time to prevent leakage of cellular components of the cell and a dissipation of ion gradients. Dissipation of ionic gradients as a result of mislocalization of membrane proteins and the overexpression of ion channels such as aquaporins have been proposed as factors leading to fluid accumulation, a characteristic of kidney cysts from patients with polycystic kidney disease (39, 40). The mechanism of fluid accumulation in the cysts is still yet to be elucidated; however, various hypotheses such as increases in adenosine triphosphate (ATP) and/or cyclic adenosine monophosphate (cAMP) levels could lead to fluid secretion (41, 42). The data presented here suggest that mislocalization or excessive openings of PC2 channels can now be added to the list of factors leading to fluid accumulation. When the PC2 channel is not in its closed conformation, the contents of the cell could be compromised, thus contributing, at least in part, to the fluid accumulation observed in the kidney cysts of patients with polycystic kidney disease.

**Acknowledgments**—We thank Dr. Stefan Somlo and Dr. Yiqiang Cai for providing us the LLC-PK<sub>1</sub> cells. We appreciate thoughtful comments on the manuscript from Dr. James Howe, Dr. Anurag Varshney, Craig Gibson, and Eva Winkler.

#### REFERENCES

- Wu, G., and Somlo, S. (2000) *Mol. Genet. Metab.* **69**, 1–15
- Wilson, P. D. (2004) *N. Engl. J. Med.* **350**, 151–164
- Wu, G., Mochizuki, T., Le, T. C., Cai, Y., Hayashi, T., Reynolds, D. M., and Somlo, S. (1997) *Genomics* **45**, 220–223
- Ikedo, M., and Guggino, W. B. (2002) *Curr. Opin. Nephrol. Hypertens.* **11**, 539–545
- Gonzalez-Perrett, S., Kim, K., Ibarra, C., Damiano, A. E., Zotta, E., Batelli, M., Harris, P. C., Reisin, I. L., Arnaout, M. A., and Cantiello, H. F. (2001) *Proc. Natl. Acad. Sci. U. S. A.* **98**, 1182–1187
- Koulen, P., Cai, Y., Geng, L., Maeda, Y., Nishimura, S., Witzgall, R., Ehrlich, B. E., and Somlo, S. (2002) *Nat. Cell Biol.* **4**, 191–197
- Clapham, D. E. (2003) *Nature* **426**, 517–524
- Hanaoka, K., Qian, F., Boletta, A., Bhunia, A. K., Piontek, K., Tsiokas, L., Sukhatme, V. P., Guggino, W. B., and Germino, G. G. (2000) *Nature* **408**, 990–994
- Qian, F., Germino, F. J., Cai, Y., Zhang, X., Somlo, S., and Germino, G. G. (1997) *Nat. Genet.* **16**, 179–183
- Tsiokas, L., Kim, E., Arnould, T., Sukhatme, V. P., and Walz, G. (1997) *Proc. Natl. Acad. Sci. U. S. A.* **94**, 6965–6970
- Anyatonwu, G. I., Buck, E. D., and Ehrlich, B. E. (2003) *J. Biol. Chem.* **278**, 45528–45538
- Jiang, Y., Lee, A., Chen, J., Cadene, M., Chait, B. T., and MacKinnon, R. (2002) *Nature* **417**, 523–526
- Tinker, A., and Williams, A. J. (1993) *Biophys. J.* **65**, 1678–1683
- Voets, T., Janssens, A., Droogmans, G., and Nilius, B. (2004) *J. Biol. Chem.* **279**, 15223–15230
- Cai, Y., Maeda, Y., Cedzich, A., Torres, V. E., Wu, G., Hayashi, T., Mochizuki, T., Park, J. H., Witzgall, R., and Somlo, S. (1999) *J. Biol. Chem.* **274**, 28557–28565
- Kim, D. H., Ohnishi, S. T., and Ikemoto, N. (1983) *J. Biol. Chem.* **258**, 9662–9668
- Ehrlich, B. E., and Watras, J. (1988) *Nature* **336**, 583–586
- Hille, B. (2001) *Ion Channel of Excitable Membranes*, 3rd Ed., p. 21, Sinauer Associates, Inc., Sunderland, MA
- Lindsay, A. R. G., Manning, S. D., and Williams, A. J. (1991) *J. Physiol. (Lond.)* **439**, 463–480
- Ohki, G., Miyoshi, T., Murata, M., Ishibashi, K., Imai, M., and Suzuki, M. (2000) *J. Biol. Chem.* **275**, 39055–39060
- Cai, Y., Anyatonwu, G., Okuhara, D., Lee, K. B., Yu, Z., Onoe, T., Mei, C. L., Qian, Q., Geng, L., Witzgall, R., Ehrlich, B. E., and Somlo, S. (2004) *J. Biol. Chem.*
- Tinker, A., and Williams, A. J. (1993) *J. Gen. Physiol.* **102**, 1107–1129
- Tinker, A., Lindsay, A. R., and Williams, A. J. (1992) *Biophys. J.* **61**, 1122–1132
- Gustafsson, A. J., Ingelman-Sundberg, H., Dzabic, M., Awasum, J., Hoa, N. K., Ostenson, C. G., Pierro, C., Tedeschi, P., Woolcott, O., Chiouan, S., Lund, P. E., Larsson, O., and Islam, M. S. (2004) *FASEB J.* **2**, 301–303
- Xu, M., and Akabas, M. H. (1993) *J. Biol. Chem.* **268**, 21505–21508
- Kurz, L. L., Zuhlke, R. D., Zang, H. J., and Joho, R. H. (1995) *Biophys. J.* **68**, 900–905
- Akabas, M. H., Stauffer, D. A., Xu, M., and Karlin, A. (1992) *Science* **258**, 307–310
- Quinn, K. Q., and Ehrlich, B. E. (1997) *J. Gen. Physiol.* **109**, 255–264
- Dulhanty, A., Haarmann, C., Green, D., and Hart, J. (2000) *Antioxid. Redox Signal.* **2**, 27–34
- Mochizuki, T., Wu, G., Hayashi, T., Xenophontos, S. L., Veldhuisen, B., Saris, J. J., Reynolds, D. M., Cai, Y., Gabow, P. A., Pierides, A., Kimberling, W. J., Breuning, M. H., Deltas, C. C., Peters, D. J., and Somlo, S. (1996) *Science* **272**, 1339–1342
- Voets, T., Janssens, A., Prenen, J., Droogmans, G., and Nilius, B. (2003) *J. Gen. Physiol.* **121**, 245–260
- Jiang, Y., Lee, A., Chen, J., Cadene, M., Chait, B. T., and MacKinnon, R. (2002) *Nature* **417**, 515–522
- Raymond, L., Slatin, S. L., and Finkelstein, A. (1985) *J. Membr. Biol.* **84**, 173–181
- Zhorov, B. S., and Tikhonov, D. B. (2004) *J. Neurochem.* **88**, 782–799
- Hoenderop, J. G., Voets, T., Hoefs, S., Weidema, F., Prenen, J., Nilius, B., and Bindels, R. J. (2003) *EMBO J.* **22**, 776–785
- Perozo, E., MacKinnon, R., Bezanilla, F., and Stefani, E. (1993) *Neuron* **11**, 353–358
- Williams, A. J., West, D. J., and Sitsapesan, R. (2001) *Q. Rev. Biophys.* **34**, 61–104
- Doyle, D., Cabral, J., Pfuetzner, R., Kuo, A., Gulbis, J., Cohen, S., Chait, B., and MacKinnon, R. (1998) *Science* **280**, 69–77
- Devuyst, O., Burrow, C. R., Smith, B. L., Agre, P., Knepper, M. A., and Wilson, P. D. (1996) *Am. J. Physiol.* **271**, F169–F183
- Wilson, P. D., Devuyst, O., Li, X., Gatti, L., Falkenstein, D., Robinson, S., Fambrough, D., and Burrow, C. R. (2000) *Am. J. Pathol.* **156**, 253–268
- Hanaoka, K., and Guggino, W. B. (2000) *J. Am. Soc. Nephrol.* **11**, 1179–1187
- Schwiebert, E. M., Wallace, D. P., Braunstein, G. M., King, S. R., Peti-Peterdi, J., Hanaoka, K., Guggino, W. B., Guay-Woodford, L. M., Bell, P. D., Sullivan, L. P., Grantham, J. J., and Taylor, A. L. (2002) *Am. J. Physiol.* **282**, F763–F775
- Tarroni, P., Rossi, D., Conti, A., and Sorrentino, V. (1997) *J. Biol. Chem.* **272**, 19808–19813
- Huang, C. J., Favre, I., and Moczydlowski, E. (2000) *J. Gen. Physiol.* **115**, 435–454